LIQUID CRYSTALS, 1987, VOL. 2, NO. 1, 39–54



# A Monte Carlo simulation of the inhomogeneous Lebwohl–Lasher lattice model

by C. CHICCOLI and P. PASINI

INFN Sez. di Bologna and CNAF, Via Mazzini, 2, 40138 Bologna, Italy

and C. ZANNONI

Istituto di Chimica Fisica, Universitá, Viale Risorgimento, 4, 40136 Bologna, Italy

(*Received 16 July 1986; accepted 25 August 1986*)

A Monte Carlo computer simulation of a modified Lebwohl–Lasher model is presented. The model consists of a set of interaction centres placed at the sites of a cubic lattice. The angular part of the pair potential is a second Legendre polynomial of the relative orientation between the two particles, like that of the Lebwohl–Lasher model. Each particle interacts with its six nearest neighbours with an attractive anisotropic potential differing in strength for the four horizontal and the two vertical neighbours. Various values of the in-plane to out-of-plane coupling ratio $\delta$ have been considered, i.e. $\delta = 0{\cdot}75, 0{\cdot}5, 0{\cdot}1, 0{\cdot}0$. The latter case corresponds to the limiting situation of a two-dimensional lattice. Systems with a 1000 particles have been simulated for $\delta = 0{\cdot}75, 0{\cdot}5$ and $0{\cdot}1$ while a sample of 3600 particles has been investigated for the two-dimensional lattice. Comparisons are made with available simulations and with mean field theory. We find that the molecular field theory predictions worsen as the effective coordination number is decreased. Energy, specific heat, second and fourth rank order parameters have been evaluated for the various models. We also present, for the first time, a way of approximately reconstructing the pair distribution, $G(r_{12}, \omega_{12})$, using maximum entropy and second and fourth rank two particle order parameters.

## 1. Introduction

Lattice models play an important role in the theory of phase transitions [1–6]. This has been widely recognized for spin systems [1–6] and, more recently for systems mimicking the orientational phase transitions found in mesophases [7, 8]. In the liquid crystal field one of the most popular models is that originally due to Lebwohl and Lasher [7–17], where particles are placed on a cubic lattice and the pair potential is taken to be

$$U_{i,j} = -\varepsilon_{ij} P_2(\cos \beta_{ij}). \tag{1}$$

Here $\varepsilon_{ij}$ is a parameter expressing the strength of the attractive interaction. It is a positive constant, $\varepsilon$, for nearest neighbour particles $i$ and $j$ and zero otherwise. $\beta_{ij}$ is the angle between the symmetry axes of these two molecules. Monte Carlo computer simulations on a $30 \times 30 \times 30$ lattice indicate that the Lebwohl–Lasher model exhibits a phase transition at a dimensionless temperature $T^* = kT/\varepsilon \simeq 1{\cdot}1232$ [17]. Molecular field theory [18, 19] predicts instead, for this system, a first order phase transition at the rather higher temperature $T^*_{NI} = 1{\cdot}321$ [19]. This approximate theory is also unable to account for the closeness of the isotropic phase limiting instability temperature to the proper transition temperature [20, 21]. Apart from these shortcomings and from an overestimation of the transition temperature and entropy,

molecular field theory works reasonably well. In particular the dependence of the second rank order parameter $\langle P_2 \rangle$ on the reduced temperature $T^+ = T/T_{NI}$, predicted by molecular field theory to be a universal curve (without any adjustable parameter) is in more than reasonable agreement with experiment [19]. However, it ought to be said that this particular order parameter versus temperature curve would be obtained under fairly mild conditions with other theories as well. Indeed every theory leading to a singlet distribution of the type

$$P(\cos\beta) \propto \exp[a_2 P_2(\cos\beta)] \tag{2}$$

would produce an identical dependence of $\langle P_2 \rangle$ on $T^+$. We are thus left with the unpleasant situation of a theory that, as we know *a posteriori*, is at least partially satisfactory, but whose predictive power is difficult to assess. Here we would like to provide a test of this predictive power in a very simple and controlled situation by changing only one element in the potential. In the inhomogeneous Lebwohl–Lasher model presented in §2 the relative strength of in-plane to out-of-plane interaction is changed. We shall show how this affects molecular field predictions and how well these predictions are borne out by the simulation.

## 2. The inhomogeneous Lebwohl–Lasher model

Here we have chosen to study the generalized model with the hamiltonian

$$-U = \sum_{\langle i,j \rangle_p} (\varepsilon_\perp)_{ij} P_2(\cos\beta_{ij}) + \sum_{\langle i,j \rangle_v} (\varepsilon_\parallel)_{ij} P_2(\cos\beta_{ij}), \tag{3}$$

where the sums are extended, respectively, to the nearest neighbours in the same laboratory horizontal plane (i.e. with interparticle vector $\mathbf{r}_{ij} \parallel \mathbf{X}, \mathbf{Y}$) and to the neighbours along the vertical, $\mathbf{Z}$ axis. We shall call this the inhomogeneous Lebwohl–Lasher model, by analogy with the so-called inhomogeneous or spatially anisotropic Ising models introduced in the study of magnetism [1, 22]. As in the original Lebwohl–Lasher model in equation (1) [7] the potential is attractive. The interaction constants are positive and equal to $\varepsilon_\perp$, $\varepsilon_\parallel$ if particles $i$ and $j$ are first neighbours and zero otherwise. The parameter $\delta = \varepsilon_\parallel/\varepsilon_\perp$ gives the relative strength of the two interactions. It is clear that the model reduces to the usual Lebwohl–Lasher one when $\delta = 1$. The lowering of $\delta$ describes a weakening of the interlayer coupling. At the limit $\delta = 0$ the system becomes a collection of independent two-dimensional layers. In this limit the lattice becomes a planar version of the Lebwohl–Lasher model first examined by Mountain and Ruijgrok [11] and will be more closely investigated elsewhere [23]. In general the present model pictures therefore an inhomogeneous, multilayer, system. It is in a way an extremely simplified model for the orientational properties of a smectic liquid crystal [24]. Here the shape of the anisotropic orientational potential between the neighbouring molecules is taken to be the same both when the molecules belong to the same or to neighbouring layers, except for a weakening in the strength of the interaction. The model also assumes that the molecules are kept apart by some other mechanism, essentially as the Lebwohl–Lasher model assumes the molecular positions to be fixed by some additional mechanism to the sites of an isotropic cubic lattice. We know, of course, that in real nematics molecules are free to move more or less as in a liquid. On the other hand the spirit of the model is to concentrate on orientational features and to assume the rest to be relatively less important. Here we are just singling out in a similar way an aspect of smectics, i.e. that to a first approximation smectic molecules are distributed in layers. Of course we should stress

that there are many qualifications to go with the smectic analogy. For example, the potential depends only on relative orientations (similar on the other hand to the McMillan one [24]), so there is no possibility of director tilt and thus of distinguishing, for example, a smectic A from a smectic C. Moreover, and even more seriously, the model does not allow for changes in translational order so we are really just looking at a orientational disordering transition. Within these limitations, there are however a few interesting analogies we can make. Smectogenic molecules are often made up of a rigid core with floppy chains at the two ends. We can imagine that by changing the end substituents and making their tails longer the strength of the interaction between molecules belonging to different layers will be weakened. Correspondingly the parameter $\delta$ will be reduced up to the point where each layer becomes a quasi two-dimensional system. On an intuitive basis we might expect the character of the orientational transition to change as the dimensionality of the latter changes in this way. On the other hand, as we shall recall in §3, molecular field theory predicts that only a scaling of the energy due to the change in effective coordination number should occur. Indeed molecular field theory predicts that two lattices will have the same value of $T_K^*$ when they have the same coordination number irrespective of the dimensionality of the lattice as, for example, is the case for a three-dimensional cubic and a two-dimensional hexagonal lattice. This is particularly strange when the all-important role of lattice dimensionality in the modern theory of phase transition is remembered.

In general, molecular field theory is expected to be exact when the coordination number tends to infinity [1, 15] and each molecule interacts on the same footing with all the others in the system. It is interesting to see how the relative effectiveness of molecular field theory is modified when changing the coordination number from the value six found in the cubic lattice to other values. Luckhurst *et al.* [15] have studied a face centred Lebwohl–Lasher lattice where the coordination number is 12. It might be expected that in that instance the performance of molecular field theory is improved and indeed this is borne out by the simulations. Here the test is somewhat more severe since the effect of changing coordination number is accompanied by a move toward a descent in lattice dimension.

## 3. Mean field theory

The potential of mean torque is obtained by standard means [19] upon averaging the pair potential in equation (3). We find

$$U(\beta) = -(2\varepsilon_{\parallel} + 4\varepsilon_{\perp})\langle P_2\rangle P_2(\cos\beta), \tag{4}$$

where $\beta$ is the angle between the molecule and the director and we have assumed $\langle P_2\rangle$ to be the same throughout the sample. We can rewrite equation (4) as

$$U(\beta)/kT = -\varepsilon_{\perp}[(2\delta + 4)/kT]\langle P_2\rangle P_2(\cos\beta), \tag{5}$$

where $\delta$ is the ratio of vertical to horizontal coupling introduced previously. A comparison of this with the effective potential for the Lebwohl–Lasher model, i.e.

$$U(\beta)/kT = -(z\varepsilon/kT)\langle P_2\rangle P_2(\cos\beta), \tag{6}$$

where $z$ (here $z = 6$) is the coordination number, shows that at molecular field theory level the effect of changing the interlayer coupling is merely that of renormalizing the temperature. Instead of $kT/\varepsilon$ we have, when $\delta$ is not one, an effective reduced temperature $kT/[(2\delta + 4)\varepsilon_{\perp})]$. In particular the transition temperature is

predicted to be at $(T^*_{NI})_\delta = (T^*_{NI})_{LL}(2\delta + 4)/z$. Putting numbers in we have $(T^*_{NI})_\delta = 1{\cdot}1232(2\delta + 4)/6 = 0{\cdot}1872(2\delta + 4)$. Thus molecular field theory makes a definite prediction. Plotting $(T^*_{NI})_\delta$ against $\delta$ we should find a straight line with slope 0·374 and intercept 0·749. The character of the transition should be unchanged as $\delta$ is reduced. Even in the two-dimensional lattice limit, with $\delta = 0$, the transition properties expressed in dimensionless units should be the same.

Saying it in another way, we see that the lattice dimensionality does not play a role at mean field level, even though of course the spin dimensionality (the number of orientational degrees of freedom) does. A lattice with spin dimensionality one and lattice dimensionality one has been studied by Denham *et al.* [25]. A lattice of dimensionality two with spin dimensionality one has also been investigated [11]. As already mentioned the effective coordination number $z' = (2\delta + 4)$ is the only relevant parameter and mean field theory predicts that, for example, a bidimensional triangular lattice and a tridimensional cubic lattice should have the same thermodynamic properties. The order parameters at the transition are also predicted to be insensitive to $\delta$ and so is, for example, the dependence of $\langle P_4 \rangle$ on $\langle P_2 \rangle$.

## 4. The simulations

We have studied four systems with different values of the ratio $\delta$ of out-of-plane to in-plane coupling constant, i.e. $\delta = 0{\cdot}75, 0{\cdot}5, 0{\cdot}1$ and $0{\cdot}0$. Our previous experience with the Lebwohl–Lasher model and that of other groups indicates that a sample size of a thousand particles is sufficient to yield the properties of the simulated model with a reasonable accuracy ($\sim 2$ per cent), provided the interest is not on the immediate neighbourhood of the phase transition. We have thus chosen to study $10 \times 10 \times 10$ lattices for the three-dimensional models. The two-dimensional limit is more delicate, since it has been studied only in one case and only for sizes up to $20 \times 20$ [11]. In a separate study [23] we have now shown that a $60 \times 60$ size has essentially converged to the large size limit, so this is the size used here. A standard Monte Carlo method with periodic boundary conditions has been employed to generate equilibrium configurations. The simulation at the first temperature studied for each of the four cases was started from a completely aligned system. The simulations at the other temperatures have been normally run in cascade starting from an equilibrium configuration at a nearby lower temperature. The orientation of each particle is stored as $\cos\beta$ and $\alpha$, where $\beta$ and $\alpha$ are the spherical polar angles of the symmetry axis of each particle. The configuration of the system is thus given by the set of $N$ such orientations $\{\alpha_i, \beta_i\}$ where $N$ is the number of particles. We update one particle at a time and as usual we shall call a cycle a set of $N$ attempted moves. A new configuration is generated by choosing a particle at random out of those that we have not yet attempted to move during the current lattice sweep [17] with a simple random shuffling algorithm [26]. The orientation of the chosen particle is then changed by generating new uniformly distributed random values of the variables $\cos\beta$ and $\alpha$. A satisfactory rejection ratio is achieved for our temperature range even with these potentially large orientational jumps. In every simulation a minimum of 4000 cycles has been used for equilibrium and thus rejected when calculating averages.

Any property of interest, $A$, is evaluated at every cycle. After a certain number of cycles $m_J$ (typically between 1000 and 2000) an average $A^J$ is calculated thus effectively coarse graining the trajectory. A further grand average is then computed as the

weighted average over $M$ such supposedly uncorrelated segments

$$\langle A \rangle = (1/N_C) \sum_J^M m_J A^J, \tag{7}$$

where $N_C = \Sigma_J^M m_J$ is the total number of production cycles. The attendant weighted standard deviation from the average $\sigma_A$ is also calculated and gives the error estimates reported for order parameters and energy in tables A 1, A 2, A 3, A 4. These tables, comprising five pages, have been deposited with the British Library Document Supply Centre as a Supplementary Publication; copies may be obtained from the British Library according to the procedure described at the end of the Journal and by quoting the number SUP 16502.

We have calculated for each simulation energy, second and fourth rank order parameters and pair correlation coefficients again of second and fourth rank. The heat capacity of the system has been evaluated from the internal energy as described later.

## 5. Results and discussion

### 5.1. *Energy*

The energy of the system is calculated as a sum of pair interactions as in equation (3). The average dimensionless single particle energies $U^* = \langle U \rangle / N\varepsilon_\perp$ at the various reduced temperatures $T^* = kT/\varepsilon_\perp$ studied are shown in figure 1 for the four systems examined. The general trend of the various curves at high temperature can be understood by expanding the configurational partition function around the isotropic limit. We find for our cubic lattice

$$Z_N = (4\pi)^N [1 + N(2 + \delta^2)/(10T^{*2}) + (2 + \delta^3)/(105T^{*3}) + \ldots] \tag{8}$$

to third order in inverse temperature. Correspondingly the energy per particle is

$$\langle U \rangle / N\varepsilon_\perp = -(2 + \delta^2)/(5T^*) - (2 + \delta^3)/(35T^{*2}) - \ldots . \tag{9}$$

Thus we see that at high temperatures the curves for small $\delta$ should tend to cluster together, since $\delta^2$ is negligible compared to 2. Moreover the curves should approach $-0{\cdot}4/T^*$ in this limit. Looking at figure 1 we see that this is indeed the case. At low

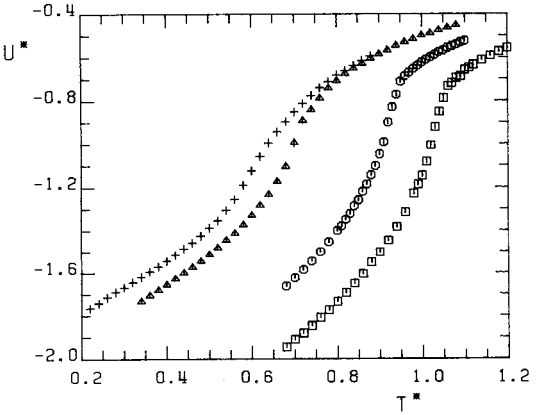


Figure 1. The single particle energy, $U^* = \langle U \rangle / N\varepsilon_\perp$, as a function of the dimensionless temperature $T^* = kT/\varepsilon_\perp$ for the Monte Carlo simulation of the inhomogeneous Lebwohl–Lasher model with $\delta = 0{\cdot}75$ (□), $0{\cdot}5$ (○), $0{\cdot}1$ (△) and $0{\cdot}0$ (+). Lattice size is $10 \times 10 \times 10$ for the first three cases and $60 \times 60$ for the last.

temperatures each curves goes to its complete order limiting value

$$\langle U \rangle / N\varepsilon_{\perp} = -\tfrac{1}{2}(2 + \delta). \tag{10}$$

### 5.2. *Heat capacity*

The heat capacity is obtained here by differentiating the average energy with respect to temperature. It is known that the differentiation of experimental or, in general, noisy data is an ill-posed problem [27]. It can be tackled through smoothing interpolation, for example, using suitable spline functions [16, 17] or by inversion methods [27]. Here we have chosen this last approach, which consists of solving the integral equation

$$U(T) = U(T_0) + \int_{T_0}^{T} dT' C_V^*(T'). \tag{11}$$

In our case energies are known at a set of temperatures, $U(T_i)$, which we can use to build an $M$ component vector of energy differences $\mathbf{u}$. We can thus write

$$\int_{(i)} dT' C_V^*(T') = u_i, \tag{12}$$

where the integral is extended to the $i$th energy interval. Choosing to calculate $C_V^*$ at a grid of K temperatures and employing a suitable numerical integration formula we reduce the integral equation to the matrix equation

$$\mathbf{WC} = \mathbf{u}, \tag{13}$$

where $\mathbf{W}$ is the weight matrix for the chosen numerical integration. $\mathbf{W}$ will of course be rectangular in normal circumstances and the problem of finding $\mathbf{C}$ is solved in terms of the generalized inverse matrix $\mathbf{W}^{\mathrm{I}}$. The generalized inverse is obtained here using the method of Rust *et al.* [28] as implemented by Lorenzutta [29]. The integration formula chosen is trapezoidal. The heat capacity was also calculated independently by interpolating and smoothing the energy data using a five point orthogonal formula before performing a standard numerical differentiation [30]. The results are similar to those found previously for our systems. The estimate of errors in heat capacity calculations is rather complicated because of the numerical schemes employed. We have thus introduced a simulation procedure as follows. First we generate a rather large number (here 100) of plausible energy versus temperature curves by sampling energy values at each temperature from a gaussian distribution of width given by the known standard deviation from the mean at that point. We then repeat the heat capacity calculation for every curve and obtain a set of $C_V^*$ values whose average and standard deviation are our final reported results. The heat capacity and standard deviation errors obtained in this way are reported on the same scale in figures 2 (*a*)–(*d*) for the various $\delta$ values. Comparing the various curves we see that in every case the heat capacity presents a peak which shifts to lower temperatures as $\delta$ decreases. We notice also that all the curves tend to $C_V^* = 1$ at low temperature, in keeping with the two degrees of freedom available to any of these systems. As the interlayer coupling becomes smaller the heat capacity peak lowers in intensity and its shape becomes broader and more symmetric. These results suggest a change in the character of transition not anticipated by molecular field theory. In figure 3 we have plotted our pseudo isotropic–nematic transition temperature, i.e. the temperature of the heat capacity anomaly maximum versus $\delta$. The Lebwohl–Lasher model result at $\delta = 1$ [17]

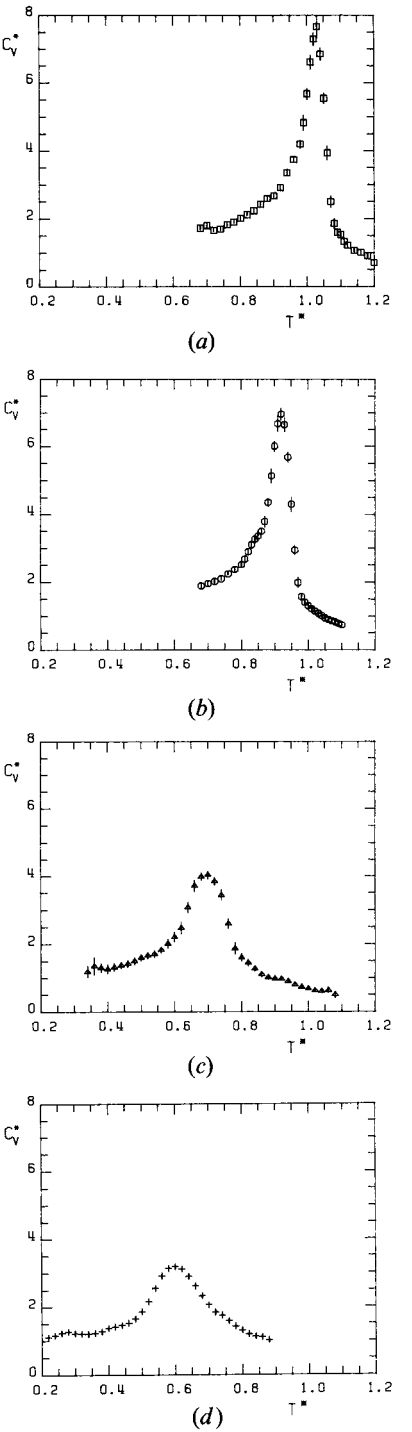


Figure 2. The heat capacity, $C_V^*$, obtained from differentiation of the energy with respect to $T^*$ as described in the text. Interaction anisotropy ratios $\delta = 0{\cdot}75$ (*a*), 0·5 (*b*), 0·1 (*c*) and 0·0 (*d*). Lattice size is $10 \times 10 \times 10$ for the first three cases and $60 \times 60$ for the last, as in figure 1.

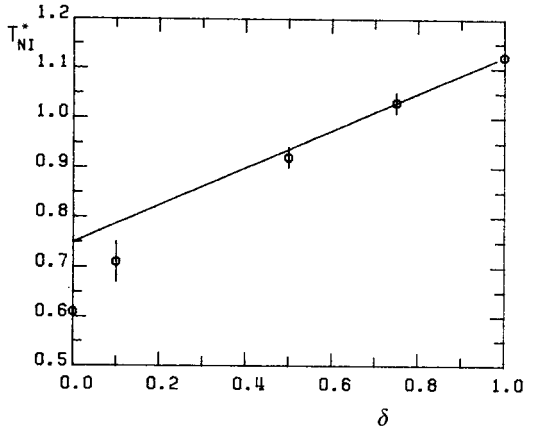


Figure 3. A plot of the temperatures where the heat capacity is a maximum, i.e. the pseudo transition temperatures, for the various $\delta$. Data are from this work except the $\delta = 1$ point which comes from [17]. The continuous line is the molecular field prediction rescaled so that it is exact at $\delta = 1$.

Transitional properties for various generalized Lebwohl–Lasher models. Here $\delta$ is the in-layer to out-of-layer coupling ratio. $z'$ is the effective nearest neighbour number, $z' = (4 + 2\delta)$. We report the pseudo transition temperatures $(T^*_{NI})_{C_v}$ and $(T^*_{NI})_D$ obtained from the heat capacity and order parameter derivative. The peak values $C^*_{max}$ and $[d\langle P_2\rangle/dT^*]_{min}$ are reported. The results correspond to a $60 \times 60$ system when $\delta = 0$ and $10 \times 10 \times 10$ systems when $\delta = 0{\cdot}1, 0{\cdot}5, 0{\cdot}75$ respectively. We also show as MFE the percentage deviation of the simulated transition temperatures from the molecular field predicted value.

| $\delta$ | $z'$ | $(T^*_{NI})_{C_v}$ | $C^*_{max}$ | $(T^*_{NI})_D$ | $[d\langle P_2\rangle/dT^*]_{min}$ | MFE (per cent) | |
|---|---|---|---|---|---|---|---|
| 0 | 4 | 0·61 ± 0·05 | 3·1 | 0·57 ± 0·05 | −4·8 | 44·4 | This work |
| 0·1 | 4·2 | 0·71 ± 0·04 | 4·0 | 0·71 ± 0·03 | −4·4 | 30·4 | This work |
| 0·5 | 5·0 | 0·92 ± 0·02 | 6·7 | 0·92 ± 0·02 | −6·8 | 19·7 | This work |
| 0·75 | 5·5 | 1·03 ± 0·02 | 7·1 | 1·03 ± 0·01 | −6·3 | 17·6 | This work |
| 1 | 6 | 1·1232 ± 0·0006 | | | | 17·6 | [17] |
| 4 | 12 | 2·43 ± 0·03 | | | | 8·7 | [15] |

has also been included and we have scaled the molecular field prediction so that it matches this case. We see that the well-known overestimation of the transition brought about by the molecular field approximation is magnified when the inter-layer coupling and thus the effective coordination number decreases. In the table we give numerical values for the heat anomaly and we also compare the percentage deviation between the transition temperatures predicted by molecular field theory and those found in this study.

### 5.3. *Order parameters*

The second rank order parameter is calculated as usual in systems with periodic boundary conditions [8, 31] from the $3 \times 3$ ordering matrix $\mathbf{Q}$, defined for a certain configuration as the sample average

$$Q_{ab} = \langle q_{i,a}q_{i,b} - \tfrac{1}{3}\rangle_S, \tag{14a}$$

$$= \frac{1}{N}\sum_{i=1}^{N} q_{i,a}q_{i,b} - \tfrac{1}{3}\delta_{a,b}; \quad a,b = x,y,z \tag{14b}$$

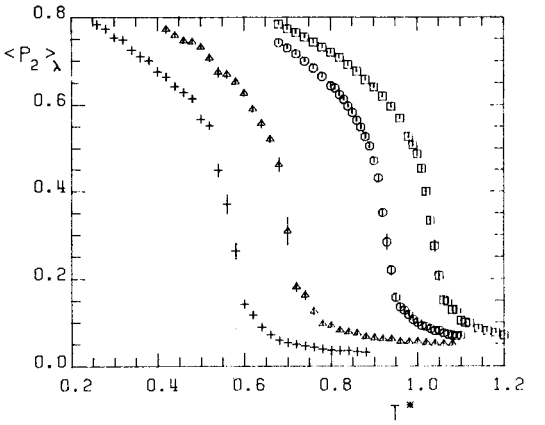


Figure 4. The second rank order parameter $\langle P_2 \rangle_\lambda$ for the four systems defined in figures 1 and 2 at temperature $T^*$. Here $\langle P_2 \rangle_\lambda$ is obtained from the largest eigenvalue of the ordering matrix as explained in the text. $\delta = 0{\cdot}75$ (□), $0{\cdot}5$ (○), $0{\cdot}1$ (△) and $0{\cdot}0$ (+).

where, for example, $q_{i,x}$ stands for the $x$ component of the unit vector $\mathbf{q}_i$ specifying the orientation of the $i$th particle and the sum is extended to all the particles in the system. More precisely an order parameter $\langle P_2 \rangle_\lambda$ has been evaluated in the present work by computing and diagonalizing $\mathbf{Q}$ at every cycle and successively averaging the largest eigenvalue, $\lambda_3$ of $\mathbf{Q}$,

$$\langle P_2 \rangle_\lambda = \tfrac{3}{2}\langle \lambda_3 \rangle. \tag{15}$$

We recall that the matrix $\mathbf{Q}$ is traceless so that $\lambda_3 \geqslant 0$ and $\langle P_2 \rangle_\lambda \geqslant 0$. The eigenvector matrix, $\mathbf{U}$, defines the transformation between the laboratory and the director coordinate frame and will be used later. The order parameters $\langle P_2 \rangle_\lambda$ obtained in this way are plotted as a function of temperature in figure 4 for the various systems studied. The order parameter is a long range property defined over the whole sample. At a true first order phase transition it falls discontinuously to zero. In our finite sample there is no bona fide discontinuity but the order parameter still changes very rapidly in the transition region. It is interesting to consider the temperature derivative of the order parameter, $D_2 = d(\langle P_2 \rangle_\lambda)/dT^*$, as a long range indicator of the transition and to compare its reponse with that of the short range indicator, i.e. of the heat capacity. We have thus computed these derivatives and their relative error estimates following the same procedure previously introduced for the heat capacity. We find the results presented in figures 5 (*a*)–(*d*). The values of the long range pseudo transition temperatures obtained are reported in the table. We see that there is excellent agreement between the long range and the short range indicators. Even for the two-dimensional system the short range and the long range indicators are within our estimated error.

We now turn to the calculation of the fourth rank order parameter $\langle P_4 \rangle$ according to the algorithm proposed in [17]. The method is based upon introducing an auxiliary fourth rank tensor $\mathbf{F}$, with components $F^M_{ijkl} = \delta_{i,z}\delta_{j,z}\delta_{k,z}\delta_{l,z}$ in the molecule fixed frame. The tensor component $F_{zzzz}$ in the director frame is, when averaged over the sample,

$$\langle F^{\mathrm{D}}_{zzzz} \rangle_{\mathrm{S}} = \langle \cos^4 \beta \rangle_{\mathrm{S}} \tag{16}$$

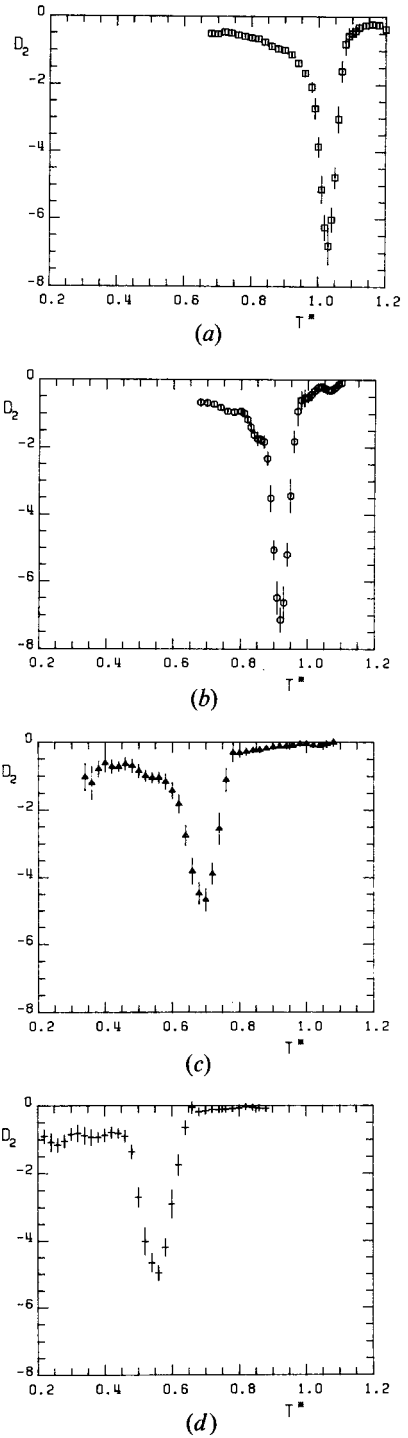


Figure 5. The temperature derivative of the second rank order parameter, $d(\langle P_2 \rangle_\lambda)/dT^*$, obtained as described in the text. Interaction anisotropy ratios $\delta = 0{\cdot}75$ (*a*), $0{\cdot}5$ (*b*), $0{\cdot}1$ (*c*) and $0{\cdot}0$ (*d*).

so that it can be used directly to compute the fourth rank Legendre polynomial average over the sample $\langle P_4 \rangle_S$ as

$$\langle P_4 \rangle_S = \tfrac{35}{8}\langle \cos^4 \beta \rangle_S - \tfrac{30}{8}\langle \cos^2 \beta \rangle_S + \tfrac{3}{8}.$$

The relevant component in the director frame is determined by first calculating at every lattice sweep the sample average of the tensor **F** in the laboratory frame as

$$\langle F^L_{abcd} \rangle_S = \langle q_a q_b q_c q_d \rangle_S \tag{18}$$

then rotating to the director frame employing the previously determined **Q** eigenvectors matrix, i.e. **U**. Thus

$$\langle F^D_{ZZZZ} \rangle_S = \sum_{a,b,c,d} U_{aZ} U_{bZ} U_{cZ} U_{dZ} \langle F^L_{abcd} \rangle_S. \tag{19}$$

This quantity is then averaged over the cycles and employed to produce the calculated $\langle P_4 \rangle_\lambda$. The values for the fourth rank order parameter obtained for our simulation are reported as a function of temperature in figure 6. We have also plotted in figure 7 the fourth rank versus the second rank order parameter for the various anisotropies. Also plotted is the curve obtained by using the distribution function in equation (2) thus in particular a Maier–Saupe type molecular field theory. We see that the curves are all relatively similar. However, the agreement with the molecular field curve is clearly much better at high $\delta$ and worsens on going towards the two-dimensional limit. Thus the mean field prediction that the dependence of $\langle P_4 \rangle$ on $\langle P_2 \rangle$ should be unchanged as the interlayer coupling is reduced is only partially verified.

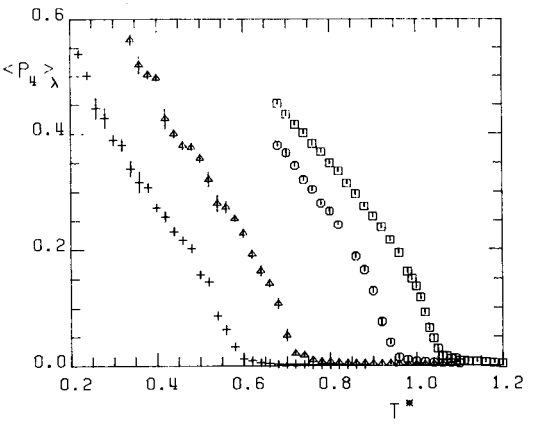


Figure 6. The fourth rank order parameter $\langle P_4 \rangle_\lambda$ obtained as described in the text plotted as a function of the reduced temperature. $\delta$ = 0·75 (□), 0·5 (○), 0·1 (△) and 0·0 (+).

### 5.4. *Orientational pair correlations*

The rotationally invariant pair distribution $G(r_{12}, \omega_{12})$ [8] determines the probability of finding two particles at distance $r_{12}$ with a certain relative orientation $\omega_{12}$. As discussed elsewhere [8] it is convenient to expand $G(r_{12}, \omega_{12})$ in a series of Legendre polynomials as

$$G(r_{12}, \omega_{12}) = G^{00}_0(r_{12}) \sum_L [(2L + 1)/64\pi^4] G_L(r_{12}) P_L(\cos \beta_{12}), \quad L \text{ even} \tag{20a}$$

$$= [G^{00}_0(r_{12})/64\pi^4]\{1 + G_2(r_{12}) P_2(\cos \beta_{12}) + G_4(r_{12}) P_4(\cos \beta_{12}) + \ldots\}, \tag{20b}$$

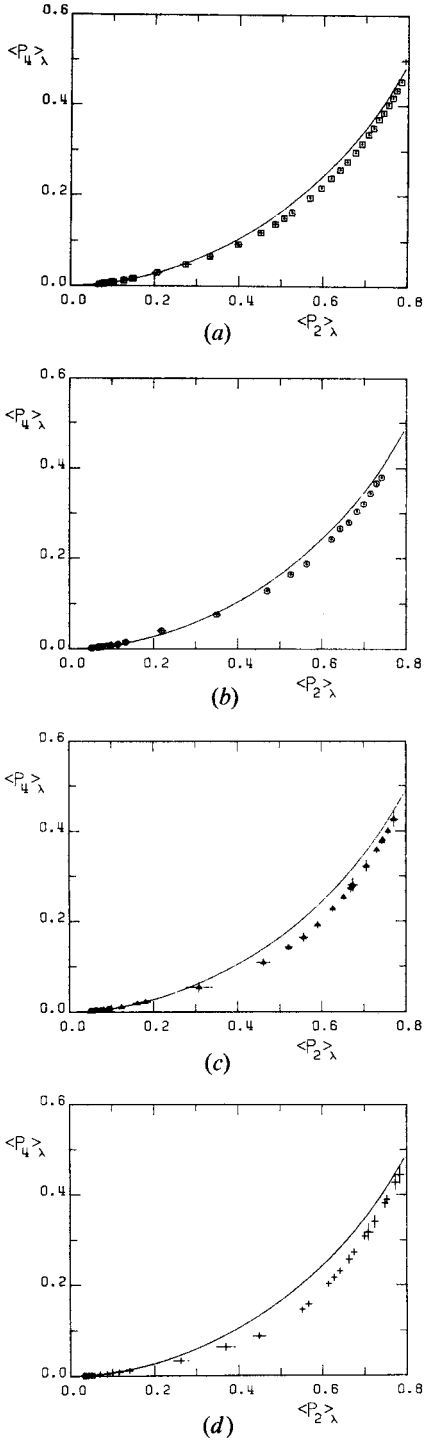


Figure 7. The fourth rank order parameter $\langle P_4 \rangle_\lambda$ obtained as described in the text plotted against the second rank order parameter $\langle P_2 \rangle_\lambda$. Also shown is the molecular field prediction (continuous line). Interaction anisotropy ratios $\delta = 0{\cdot}75$ (*a*), 0·5 (*b*), 0·1 (*c*) and 0·0 (*d*).

where $G_0^{00}(r_{12})$ is the scalar distribution of the particle centres and the expansion coefficients define two-particle order parameters. These in turn give the correlation between the orientation of two particles separated by a distance $r_{12}$

$$G_L(r_{12}) = [1/G_0^{00}(r_{12})] \int d\omega_1 \, d\omega_2 G(r_{12}, \omega_{12}) \, P_L(\cos \beta_{12}),$$
$$= \langle P_L(\cos \beta_{12}) \rangle_{r_{12}}. \tag{21}$$

For our lattice system the particle positions are fixed and their distribution is just a series of delta functions centred at the successive shell positions at distance $r_k$ from the reference particle and with a population of $z_k$ neighbours. Here we intend $r$ to be expressed in lattice units.

We have calculated the first two angular pair correlation coefficients $G_2(r)$ and $G_4(r)$ [8, 17]. In figure 8 we show $G_2(r)$ and $G_4(r)$ for three temperatures for the system

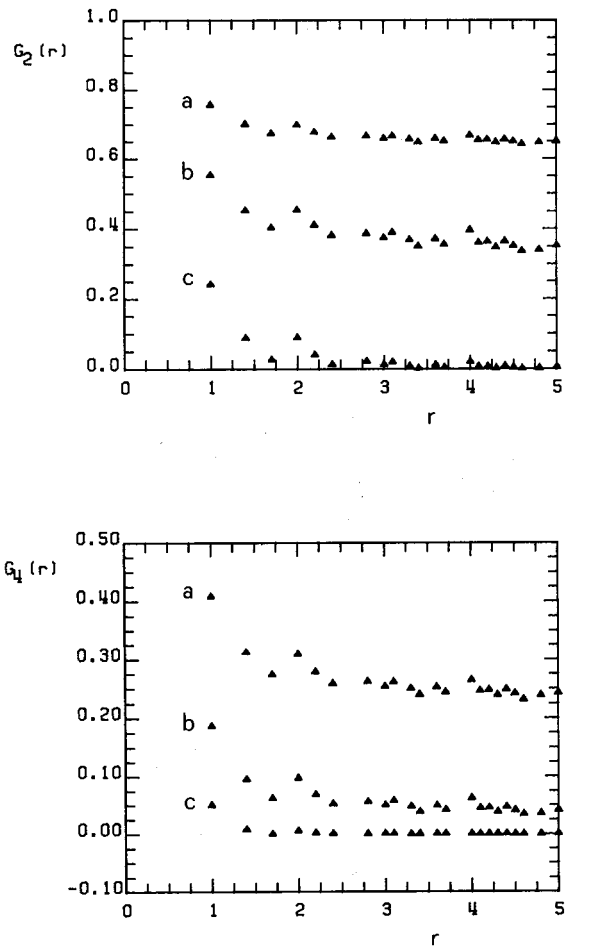


Figure 8. The second rank spatial correlation function $G_2(r)$ and its fourth rank analogue $G_4(r)$ for the inhomogeneous Lebwohl–Lasher model with anisotropy $\delta = 0{\cdot}1$. We show results at three temperatures, below and above the transition, i.e. $T^* = 0{\cdot}40$, *a*; $0{\cdot}62$, *b*; and $0{\cdot}82$, *c*.

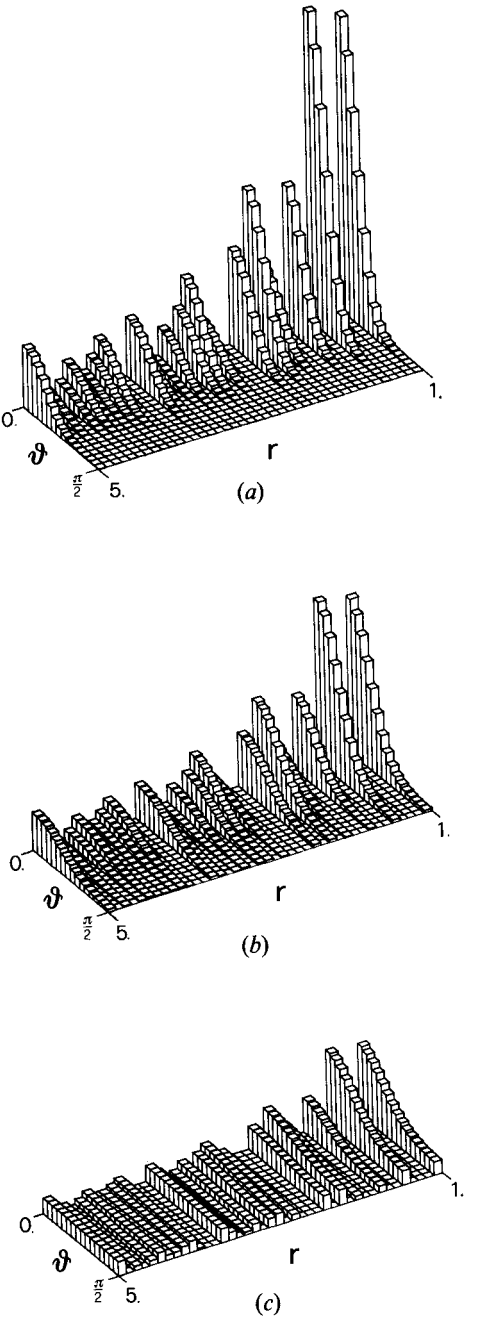


Figure 9. Histograms of the positional–orientational pair distribution $G(r_{12}, \omega_{12})$ as reconstructed from maximum entropy principles (equation (22)) for $\delta = 0{\cdot}10$. Three instances are shown, respectively at temperature $T^* = 0{\cdot}40$ (*a*), $0{\cdot}62$ (*b*) and $0{\cdot}82$ (*c*). These correspond to the $G_2(r)$ and $G_4(r)$ in figure 8.

with $\delta = 0{\cdot}1$. The curves show the expected decay respectively to a plateau or to zero when the temperature is below or above the transition. As we see from equation (20), $G_2(r)$ and $G_4(r)$ define a second rank truncation of the whole pair distribution. Although this approximation is all we need to calculate second rank and fourth rank pair properties we do not expect it to be a very good approximation to the full pair distribution on the left-hand side of equation (20). In particular a paradoxical negative probability could even be found by retaining the simple truncation. We have therefore used $G_2(r)$ and $G_4(r)$ to reconstruct the best inference for the two-particle distribution according to maximum entropy principles [16, 32] based on the second rank and fourth rank information, i.e.

$$G(r_{12}, \omega_{12}) = G_0^{00}(r_{12}) \exp[a_0 + a_2(r_{12}) P_2(\cos\beta_{12}) + a_4(r_{12}) P_4(\cos\beta_{12})]. \quad (22)$$

The coefficients $a_2$ and $a_4$ are obtained numerically by imposing the condition that at every $r_{12}$ the two point order parameters $G_2$ and $G_4$ are re-obtained by integration of equation (22). As far as we are aware this is the first such reconstruction of the pair distribution. In figure 9 we show, as an example, histograms reconstructed in this way from the three sets of $G_2(r)$ and $G_4(r)$ given in figure 8. The distributions are normalized by integration upon distances and orientations to the same constant value.

## 6. Conclusions

We have studied four systems belonging to the generalized Lebwohl–Lasher model family where the inter-layer coupling is decreased up to the limit of independent layers. We have found that the transition temperature decreases by reducing the coupling and that the reduction is progressively greater than predicted by the molecular field theory. Thus the 20 per cent in the nematic–isotropic transition temperature in the Lebwohl–Lasher model cannot be taken, in general, as a safe estimate. Moreover the transitions becomes less first order in character, while again this is not anticipated by mean field. In our investigation we have characterized the nematic phase with second and fourth order parameters. We have also proposed a way of reconstructing the pair distribution using maximum entropy techniques.

The simulations were run on a DEC VAX 11-780 minicomputer at Istituto di Fisica, INFN, and on a VAX 11-780 and VAX 11-725 at Istituto di Chimica Fisica. C.Z. thanks C.N.R. and Min.P.I. (Rome) for grants towards the cost and maintenance of the latter systems.

## References

[1] STANLEY, H. E., 1971, *Introduction to Phase Transitions and Critical Phenomena* (Oxford University Press).

[2] DOMB, C., and GREEN, M. S., 1972, *Phase Transitions and Critical Phenomena* (Academic Press).

[3] BINDER, K., 1979, *Monte Carlo Methods in Statistical Physics*, edited by K. Binder (Springer-Verlag), Chap. 1, and references therein.

[4] LANDAU, D. P., 1984, *Applications of the Monte Carlo Method in Statistical Physics*, edited by K. Binder (Springer-Verlag), Chap. 3, and references therein.

[5] MOURITSEN, O. G., 1984, *Computer Studies of Phase Transitions and Critical Phenomena* (Springer-Verlag).

[6] BINDER, K., 1985, *J. comp. Phys.*, **59**, 1.

[7] LEBWOHL, P. A., and LASHER, G., 1972, *Phys. Rev.* A, **6**, 426.

[8] ZANNONI, C., 1979, *The Molecular Physics of Liquid Crystals*, edited by G. R. Luckhurst and G. W. Gray (Academic Press), (a) Chap. 3, (b) Chap. 9.

[9] JANSEN, H. J. F., VERTOGEN, G., and YPMA, J. G. J., 1977, *Molec. Crystals liq. Crystals*, **38**, 87.
[10] MEIROVITCH, H., 1976, *Chem. Phys.*, **21**, 251.
[11] MOUNTAIN, R., and RUIJGROK, TH. W., 1977, *Physica* A, **89**, 522.
[12] ZANNONI, C., and GUERRA, M., 1981, *Molec. Phys.*, **44**, 849.
[13] HUMPHRIES, R. L., and LUCKHURST, G. R., 1982, *Proc. R. Soc.* A, **382**, 307.
[14] LUCKHURST, G. R., and SIMPSON, P., 1982, *Molec. Phys.*, **47**, 251.
[15] LUCKHURST, G. R., ROMANO, S., and SIMPSON, P., 1982, *Chem. Phys.*, **73**, 337.
[16] ZANNONI, C., 1985, *J. chem. Phys.*, **84**, 424.
[17] FABBRI, U., and ZANNONI, C., 1986, *Molec. Phys.*, **59**, 763.
[18] MAIER, W., and SAUPE, A., 1958, *Z. Naturf.* A, **13**, 1958.
[19] LUCKHURST, G. R., 1979, *The Molecular Physics of Liquid Crystals*, edited by G. R. Luckhurst and G. W. Gray (Academic Press), Chap. 4.
[20] STINSON, T. W., and LITSTER, J. D., 1970, *Phys. Rev. Lett..*, **25**, 503.
[21] SLUCKIN, T. J., 1983, *Molec. Phys.*, **49**, 221.
[22] LANDAU, D. P., 1976, *Phys. Rev.* A, **24**, 5156.
[23] CHICCOLI, C., PASINI, P., and ZANNONI, C. (to be published).
[24] MCMILLAN, W. L., 1972, *Phys. Rev.* A, **6**, 936.
[25] DENHAM, J. Y., HUMPHRIES, R. L., and LUCKHURST, G. R., 1977, *Molec. Crystals liq. Crystals*, **41**, 67.
[26] KNUTH, D. E., 1981, *The Art of Computer Programming*, Vol. 2 (Addison-Wesley).
[27] TIKHONOV, A., and ARSENINE, V., 1976, *Methodes de resolution de problemes mal poses* (MIR).
[28] RUST, B., BURRUS, W. R., and SCHNEEBERGER, C., 1966, *Comms. ACM*, **9**, 381.
[29] LORENZUTTA, S., 1967, Un metodo di inversione generalizzata per la soluzione di sistemi lineari. CNEN Report CEC 67, p. 16.
[30] ABRAMOWITZ, M., and STEGUN, I. A. (editors), 1964, *Handbook of Mathematical Functions* (Dover).
[31] VIELLARD-BARRON, J., 1974, *Molec. Phys.*, **28**, 809.
[32] LEVINE, R. D., and TRIBUS, M., 1978, *The Maximum Entropy Formalism* (MIT Press).